Monolith Catalytic Process for Producing Sorbitol: Catalyst Development and Evaluation

Robert R. Broekhuis,* Bridgette M. Budhlall, and Andrew F. Nordquist

Air Products and Chemicals, Inc., 7201 Hamilton Boulevard, Allentown, Pennsylvania 18195

Monolithic ruthenium catalysts (Ru/inorganic washcoat/cordierite) were evaluated for use in a monolith loop reactor process for hydrogenating glucose to sorbitol. Washcoat formulations included alumina, silica, titania, zirconia, and selected mixed oxides. Commercially attractive reaction rates were attained with several catalysts. Rates normalized to the amount of Ru were lower for monolithic catalysts than for Ru/C slurry catalyst benchmarks, most likely because of internal mass-transfer limitation. The concentrations of reaction byproducts (gluconic acid, ethylene glycol, and mannitol) were analyzed by high-performance liquid chromatography and are compared to slurry benchmarks. Selected monolithic catalysts exhibited a slow but steady activity decline in extended life testing (tens of runs); the deactivation mechanism has not yet been elucidated. With some further catalyst optimization, monolith catalysts can successfully replace the Raney nickel catalysts currently in use at the commercial scale, lower the overall catalyst cost, and reduce metal leaching into the reaction product.

Introduction

Monoliths have been used in gas-phase catalytic applications for many years. They are particularly prevalent in mobile and stationary environmental application areas, including automotive exhaust catalysts. The use of monoliths to catalyze gas−liquid reactions is not as widespread, but the area has attracted considerable academic interest for over 10 years. As a class of gas−liquid reactions, hydrogenations have attracted the most interest, especially those currently conducted in slurry reactors. Cybulski et al.[1] compare monolith reactors to slurry reactors in a modeling analysis. Advantages of monolith reactors over batch stirred-tank slurry reactors include a substantial decrease in catalyst handling, more flexibility in design and scale-up, and the elimination of certain selectivity problems associated with batch slurry reactor operations. Heiszwolf et al.[2] propose a monolith loop reactor in which liquid is circulated through the monolith reactor by means of a pump-around loop, using traditional liquid distribution devices such as spray nozzles. Gas is introduced into the reactor by gravity-driven natural circulation. A batch hydrogenation is conducted by continuously circulating liquid through the monolith until conversion is complete; the conversion per pass is typically small.

A similar concept is the patented monolith loop reactor technology,[3] which combines the concept of a monolith loop reactor with gas−liquid ejector technology, in which the ejector replaces the traditional liquid distribution device. Compared to a gravity-driven monolith reactor, greater superficial velocities through the monolith channels can be attained, resulting in higher rates of mass transfer and reaction. An analysis of the pressure drop and mass transfer through ejector-driven monolith reactors is presented by Broekhuis et al.[4]

Sorbitol is a large-scale industrial product with applications primarily in foods, personal care, and vitamin C production, with an annual global production exceeding 700 000 metric tons. It is produced by hydrogenating aqueous glucose solutions derived by hydrolyzing natural starches, using a Raney nickel catalyst in batch slurry reactors operated at pressures of 6−20 MPa and temperatures of 393−423 K. The catalyst is maintained in the reactor by gravity settling between batches, with a portion of the catalyst replaced to make up for mechanical and physical activity losses. Significant concentrations (tens of ppm) of nickel leach into the product solution and must be removed by ion exchange. In many cases, disposal of the nickel is becoming an environmental concern.

Academic and industrial studies have demonstrated the effectiveness of ruthenium-based catalysts for sugar hydrogenations. Ruthenium has a higher activity than nickel (or can be used at lower temperatures) and leaches to a much smaller extent. Currently, ruthenium catalysts are used in certain specialty applications, but Raney nickel remains the industrial catalyst for large-scale sorbitol processes. Challenges using a slurry ruthenium catalyst include the higher cost of ruthenium compared to nickel and the low density of supported ruthenium catalyst particles compared to Raney nickel, which makes settling of the catalyst between batches impractical and gives rise to the need for a more extensive filtration capacity.

These challenges can be addressed by using a monolithic ruthenium catalyst. Immobilizing the ruthenium on a monolithic support can increase the overall catalyst life in the process, thereby reducing catalyst replacement costs even when using a more expensive catalytic metal. The monolith reactor retains the catalyst in fixed form, so that no filtration is required. Therefore, sorbitol production poses a relevant case study for the monolith loop reactor concept. We will report our efforts to characterize the performance of monolithic catalysts in this application at commercially relevant conditions. Of particular interest are the effects of process parameters (temperature, pressure, and glucose concentration) on the catalyst activity, selectivity, and stability.

Process Chemistry

Structures of the sugars and their derivatives discussed here are shown in Figure 1. In the desired

* To whom correspondence should be addressed. E-mail: broekhrr@airproducts.com.

10.1021/ie0400393 CCC: $27.50
Published on Web 07/15/2004

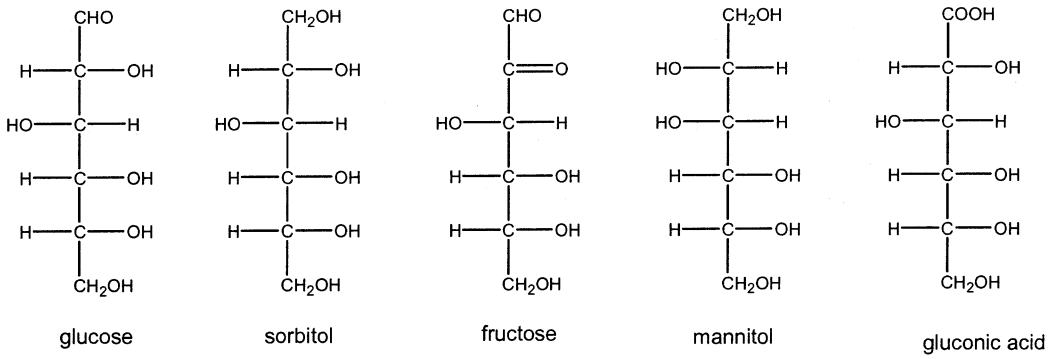

Figure 1. Structures of the hexoses and derivatives discussed in this paper.

reaction, D-glucose in an aqueous solution is converted to D-sorbitol. Glucose can undergo various other reactions: alkaline conditions catalyze both the isomerization to fructose and the dehydrogenation to gluconic acid;[5] high temperatures lead to various higher-molecular-weight products of caramelization reactions; it may isomerize to other monosaccharides.

Common byproducts of the hydrogenation reaction are cracking/hydrogenolysis products such as ethylene glycol and glycerol. In addition, some of the homogeneous byproducts are converted to their hydrogenated forms. Most notably, fructose is hydrogenated to a mixture of 55−60% sorbitol and 40−45% mannitol. Other possible sugar alcohol byproducts include iditol and galactitol.

To avoid excessive catalyst leaching and alkaline-catalyzed side reactions, the pH of the glucose feedstock is typically adjusted to $5.5 < \text{pH} < 6.5$ in industrial processes, by adding small amounts of acids or bases.

Many mechanisms and models have been proposed in the glucose hydrogenation literature. Crezee et al.,[6] who include a useful review of the literature, describe their results using Ru/C slurry catalysts. They could adequately fit their rate profiles with three Langmuir−Hinshelwood−Hougen−Watson (LHHW)-type models. In all models, they ignore hydrogen adsorption terms in the denominator because they found that rates were proportional to hydrogen pressure. Each of the models is of the form

$$r_{H_2} = \frac{k_r K_G c_G p_{H_2}}{(1 + K_G c_G)^n} \qquad c_G = c_{G0}(1 - \xi) \tag{1}$$

where the exponent n takes a value of 1, 2, or 3. k_r is a lumped parameter (the product of kinetic and equilibrium constants), K_G the glucose adsorption constant, c_{G0} the initial glucose concentration, and ξ the fractional conversion. This expression corresponds to the physical mechanism in which glucose adsorption is at dynamic equilibrium and the rate-determining step is the reaction between adsorbed glucose and hydrogen. Hydrogen is adsorbed noncompetitively ($n = 1$) or adsorbed on the same sites as glucose, either molecularly ($n = 2$) or dissociatively ($n = 3$). The authors could not distinguish the models using their data.

We will express the temperature dependence of lumped parameter k_r in terms of an apparent activation energy, using the standard operating temperature (393 K) as a reference temperature:

$$k_r = k_{r,393}\exp\left[\frac{E_A}{R}\left(\frac{1}{393} - \frac{1}{T}\right)\right] \tag{2}$$

The effect of temperature on K_G can be expressed similarly, using heat of adsorption rather than activation energy.

Catalysts

While some work on inorganically supported ruthenium catalysts has been reported, most studies of ruthenium catalysis for glucose hydrogenation have used carbon-supported ruthenium. Hence, we will benchmark monolithic catalysts against Ru/C slurry catalysts. Various forms of carbonaceous or carbon-coated monolithic supports have been developed and described in recent years. However, we have found in several applications that none of these can match carbon-supported slurry catalysts in activity, selectivity, or stability. Until better formulations become available, we have chosen instead to evaluate ruthenium catalysts supported on inorganic washcoat materials. Suitable materials include alumina, silica, titania, and zirconia in their various crystalline phases, as well as mixed oxide formulations.

Cordierite monolithic structures with 400 channels/in.^{2} were used as the mechanical support. Various washcoat materials were applied at a loading of 100−200 kg/m^3 monolith according to customary procedures,[7] after which the ruthenium active metal (nonhalide precursor) was deposited onto the washcoat material, again following typical catalyst preparation procedures. After drying and/or calcination, the monolithic catalysts were reduced in a hydrogen-containing gas at 300 °C and passivated in dilute oxygen at room temperature.

For all washcoat formulations, ruthenium was applied at a loading of 17.7 kg/m^3 monolith. For one washcoat formulation, ruthenium loadings of 3.2 and 9.4 kg/m^3 were also prepared.

Chemicals

The glucose feedstock was reagent-quality crystalline D-glucose (anhydrous or monohydrate) from Aldrich or Fischer. Besides traces (<0.02 wt %) of gluconic acid (which may have formed after dissolving the glucose), no impurities were detected in these materials. Their 40 wt % solutions in deionized water exhibited pH levels in the 5.5−6.5 range and were used without pH adjustment. To avoid the formation of gluconic acid due to dissolved oxygen,[8] the deionized water was in most cases deoxygenated by prolonged sparging with nitrogen. However, no difference was observed between runs conducted with and without this precaution. Industrial sorbitol processes use refined cornstarch hydrolysates as the glucose feedstock. In these feedstocks, glucose

accounts for 97−99% of the solids, the remainder being maltose, maltotriose, fructose, and other saccharides. Experiments using such feedstocks were conducted at the pilot scale and will be reported elsewhere.

Equipment and Methods

Laboratory experiments were conducted using a Mettler RC1e reaction calorimeter, in an HP100 stainless steel reactor. Cylindrical monolith elements (0.05 m × 0.05 m) were tested in a specially designed holder, with upward gas−liquid flow through the monolith induced by an impeller designed to match the holder. A Büchi Pressflow gas controller delivered hydrogen gas to the reactor, to maintain a constant pressure and quantify the hydrogen uptake rate. Standard operating conditions were temperature 393 K, pressure 8.1 MPa, and agitation speed 1800 rpm; deviations from these standard conditions are noted where applicable. Glucose solutions were charged to the reactor at room temperature and rapidly heated (<30 min) to the desired temperature under hydrogen pressure. With the exception of a few experiments designed to track byproduct formation, reactions were terminated 10−15 min after the hydrogen uptake slowed to a trickle, by initiating a rapid cooldown.

Several experiments were conducted using a recycling flow loop, in which a hydrogen-saturated reaction solution was circulated through an external tubular reactor containing a monolith stack (0.2 m length × 0.025 m diameter) at a flow rate of 10 L/min. This mode of operation, with low conversion per pass, more closely resembles the envisioned industrial implementation.

Final products and, in several experiments, intermediate samples were analyzed using a Waters Alliance high-performance liquid chromatograph (HPLC) with a Sugar Pak I Ca^{2+} ion-exchange resin column (20 A, 6.5 mm i.d. × 300 mm length) and a differential refractive index detector. HPLC conditions were as follows. Column temperature: maintained at 363 K using a water bath. Mobile phase: 100 mg/L calcium disodium−ethylenediaminetetraacetic acid buffer in HPLC-grade water, flowing at 0.5 mL/min. Injection volume: 20 μL. Sample analysis time: 20 min. Glucose, sorbitol, gluconic acid, fructose, ethylene glycol, and mannitol were quantified using this method. Mannitol coelutes with glycerol; in our analysis we attribute the entire peak to mannitol. Several additional impurities and byproducts were observed but not identified or quantified.

Glucose concentrations for some samples were determined using an enzymatic glucose assay kit (Sigma-Aldrich, Inc., product GAGO-20). The colorimetric method uses glucose oxidase, peroxidase, and *o*-dianisidine reagents to produce a linear absorbance response on a spectrophotometer at 540 nm.

The concentrations of metal ions present in selected samples were determined using inductively coupled plasma optical emission spectroscopy with a Perkin-Elmer OPTIMA 3000 DV instrument.

Reaction Rates

Definitions. Because both the catalyst cost and reactor design are most closely tied to the volume of the catalyst, we express reaction rates for glucose hydrogenation in terms of moles of hydrogen converted per cubic meter of monolithic catalyst per second, mol/m^3·s. Where monolithic catalyst rates are compared with slurry catalysts, both are normalized to the amount of ruthenium: mol/kg$_{Ru}$·s. The reaction rate varies with the degree of conversion during a batch. The measure typically used to quantify batch reaction performance is the mid-conversion rate, $r_{H_2,50\%}$. To eliminate the effects of experimental scatter, the rate profile is averaged across the 40−60% conversion range. The peak rate, which occurs at lower conversion, is higher than $r_{H_2,50\%}$, whereas rates drop to much lower levels during the final stages of conversion, where the rate varies linearly with the glucose concentration.

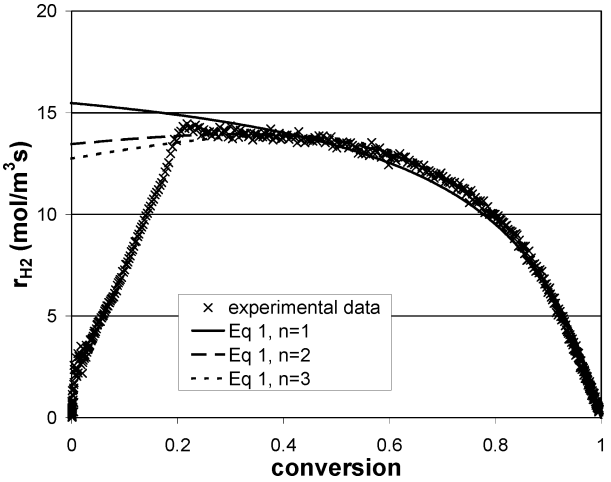

Figure 2. Rate profile for a typical monolith-catalyzed glucose hydrogenation experiment (catalyst HH, 393 K, 8.1 MPa, and c_{G0} = 2.61 mol/L). The initial part of the curve reflects increasing rate as the temperature ramps from ambient to its setpoint. The best fit of eq 1 to the data is also plotted, for $n = 1-3$.

To examine the kinetics of the reaction, the raw data expressed in terms of rate vs time must be converted to rate vs conversion. The conversion is calculated by mass balance from the hydrogen uptake, corrected for the amount of hydrogen in the reactor headspace as a function of temperature and pressure. The hydrogen mass balance closed to within 5%.

Figure 2 shows the results of a typical experiment expressed as rate vs conversion. The shape of the rate profile is similar for all experiments: nearly flat at the beginning of the batch (after the reaction temperature is attained) and transitioning into nearly linear toward the end of the batch, implying a first-order dependence on the glucose concentration. This rate profile may be affected by the kinetics and mechanism of reaction, adsorption equilibria, and external or intraparticle mass transfer. External mass-transfer effects, however, are less likely to affect the first-order part of the profile, where reaction rates are slow. Therefore, the slope of the final linear dependence, evaluated between 90% and 100% conversion, is a useful secondary measure of the reaction rate:

$$k_1 = -\frac{\mathrm{d}r_{H_2}}{c_{G0}\,\mathrm{d}\xi} \tag{3}$$

In the design of a production process, for a given production rate the reactor size (and, therefore, the catalyst cost) is inversely proportional to the reaction rate achieved by this reactor and catalyst. The rate, in this case, is the amount of sorbitol produced divided by the duration of the batch cycle, which includes filling, heatup, cooldown, and emptying/filtration times. A simple economic analysis suggests that monolith-based

processes can be commercially attractive when the monolith reactor volume is 5−10% of the liquid batch volume and the catalyst can sustain the desired rate for several hundred consecutive batches.[9] This, in turn, translates to an approximate rate target of $r_{H_2,50\%} > 10$ mol/m^3·s, given the typical shape of the rate vs conversion profile.

Effect of the Pressure and Agitation Rate. Preliminary experiments were conducted to evaluate the effects of the pressure and agitation rate on the rate of reaction. Experiments in the pressure range of 1.5−6 MPa (T = 393 K; c_{G0} = 2.61 and 3.70 mol/L) demonstrated that the reaction rate was proportional to the hydrogen pressure applied, as would be predicted by eq 1.

To assess the degree to which external mass transfer affects the hydrogenation rate under laboratory conditions, the agitation rate was varied between 1600 and 2100 rpm in experiments using 2.6 and 3.7 mol/L glucose. The agitation rate did not significantly affect the reaction rate at the higher concentration; at the lower initial concentration, a plateau in the reaction rate was reached for agitation rate > 1700 rpm. Because our experiments were conducted at 1800 rpm, we conclude that our results reflect the best mass-transfer and mixing rates that can be achieved in our laboratory reactors. For a meaningful analysis of mass-transfer effects, it would be necessary to understand how the liquid and gas flow rates through the monolith vary as a function of the agitation rate and liquid viscosity. Because these relationships have not been established, we cannot conclude that external mass-transfer limitations are avoided. However, other hydrogenation reactions conducted in the same equipment proceeded at much faster rates; even allowing for lower mass-transfer rates due to lower hydrogen solubility and higher viscosity, we would expect external mass transfer for the current experiments to be relatively fast compared to the rates of reaction. Certainly at the end of the batch, when the reaction rates are low, the overall rate should be governed by the rates of internal mass transfer and kinetics.

Effect of the Circulation Mode. Most experiments were conducted using the monolith holder mounted inside the HP100 reactor, with upward flow induced by a custom agitator. This equipment has been shown, using fast nitroaromatic hydrogenation reactions, to be able to sustain reaction rates (and, therefore, mass-transfer rates) well above the reaction rates measured for glucose hydrogenation. However, the effect of the rather higher viscosity of the glucose/sorbitol solutions on the effectiveness of this equipment was not well understood. A greatly decreased flow velocity through the monolith would result in significant external mass-transfer limitations. To assess this, monolithic catalysts were also tested in an external flow loop where the flow velocity could be independently controlled. The flow velocity in this configuration was greater than 0.4 m/s, which is almost certainly faster than that in the holder configuration and within the design velocity range for commercial implementation.

An external-loop experiment at standard conditions using catalyst F yielded rate measures that were similar to the ones obtained using the holder, within the range of experimental error. Because the rate did not significantly increase upon increasing the flow velocity, we conclude that external mass transfer is unlikely to be an important factor in the overall reaction rate.

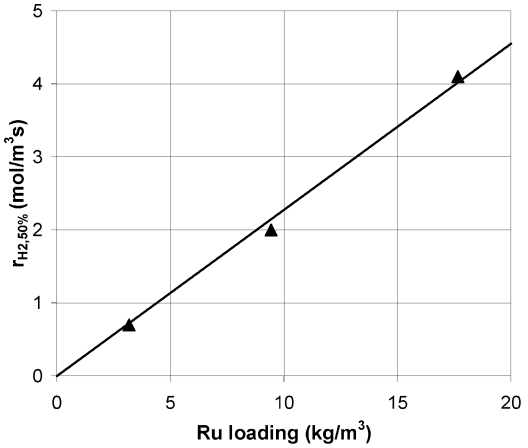

Figure 3. Relative rates of glucose hydrogenation for catalyst A at three Ru loadings. Experiments at 373 K, 6.3 MPa, and c_{G0} = 2.61 mol/L.

Effect of Ruthenium Loading. One washcoat formulation was prepared with three different ruthenium loadings: 3.2, 9.4, and 17.7 kg/m^3. All three were used in batch experiments at 373 K and 6.1 MPa. Surprisingly, Figure 3 shows that the dependence of the rate on loading was very nearly linear. This suggests that the metal dispersion is as high at the very high loading level of 17.7 kg/m^3 as it is at the more moderate level of 3.2 kg/m^3. Also, we might infer from the results that mass transfer (even intraparticle) does not affect the overall reaction rates at the conditions of these experiments. Both conclusions seem contrary to expectations, so we wish not to infer too much from three isolated experiments. However, it is clear that high ruthenium loadings are beneficial. All further experiments were conducted at the highest loading level. Even higher ruthenium loadings should be explored to determine the economic optimum loading as a function of ruthenium metal pricing, monolith manufacturing cost, and process parameters.

Effect of the Washcoat Formulation. Each of the catalysts was evaluated in one or more experiments conducted at standard conditions of 2.61 mol/L glucose, 393 K, and 6.3 and/or 8.1 MPa. For each experiment, the two rate performance measures defined above ($r_{H_2,50\%}$ and k_1) were determined and, where appropriate, adjusted to a common pressure of 8.1 MPa assuming a linear dependence on the hydrogen partial pressure. For each catalyst, the experiment showing the best overall performance was selected. The results are given in Table 1 and Figure 4. The figure shows that the two measures of catalyst activity correlate well. All catalysts demonstrate a significant activity toward glucose hydrogenation, with the relative difference between the best- and worst-performing catalyst being less than 50%. Among the highest-performing catalysts were formulations based on silica, titania, and zirconia.

The Brunauer−Emmett−Teller (BET) surface areas (39−164 m^2/g) and average pore diameters (68−184 Å) were measured for each of the catalysts. No correlation between these physical parameters and the hydrogenation activity could be discerned.

Effect of the Calcination Procedure. Vanoppen et al.[10] suggest that increased activity might be achieved by replacing the ruthenium precursor calcination step during catalyst preparation with a low-temperature

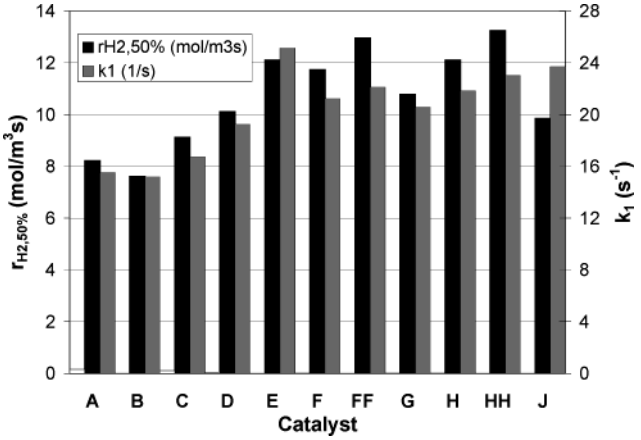

Figure 4. Rate performance measures for each of the monolithic catalysts (see Table 1). The two activity measures are discussed in the text. For each catalyst, results from the best-performing run at 393 K are plotted, with rates normalized to 8.1 MPa.

Table 1. Overview of Catalysts, Their Washcoat Constituents, and Their Rate Performance Measures[a]

catalyst	washcoat	$r_{H_2,50\%}$ (mol/m^3·s)	k_1 (s^{-1})
A	alumina	8.2	15.5
B	alumina	7.6	15.2
C	mixed	9.1	16.8
D	mixed	10.1	19.3
E	silica	12.1	25.1
F	titania	11.8	21.2
FF	titania	13.0	22.1
G	titania	10.8	20.6
H	zirconia	12.1	21.8
HH	zirconia	13.3	23.0
J	zirconia	9.9	23.7

[a] All catalysts were prepared by Johnson Matthey.

drying step. Two catalysts that showed high performance in their calcined versions (F and H) were prepared accordingly (FF and HH) and evaluated according to the same procedure. The BET surface areas of the noncalcined materials were similar to their calcined equivalents. Pore diameters are somewhat smaller for the noncalcined catalysts.

The noncalcined catalysts, upon initial evaluation, showed considerably lower activity than their calcined equivalents. However, their performance continued to improve with each successive run, until the 10th run or so, after which the performance reached a plateau. The best performance of the noncalcined catalysts was somewhat better than that of the calcined equivalents. Apparently, the catalysts as prepared had not yet reached their most-active configuration. This could be due to the presence of the ruthenium precursor material in the finished catalyst and/or lower reduction effectiveness for the precursor-laden (dried but not calcined) monolith. However, subsequent thermogravimetric analysis of the noncalcined catalyst showed no weight loss that could be attributed to the residual precursor.

Several (calcined as well as noncalcined) catalyst formulations displayed sufficient activity (>10 mol/m^3·s) to render a monolith-based process for sorbitol commercially attractive. Further optimization of the catalysts (changes in washcoat materials, ruthenium loading, ruthenium precursors, calcination, and/or reduction treatments) would likely result in even higher activity.

Effect of the Temperature. The effect of the temperature is evident from every batch experiment: the rate increases as the temperature is ramped up at the beginning of the experiment. Even though rate calculations during temperature ramp-up are complicated by the corrections for headspace gas expansion and water vapor pressure, the Arrhenius plot constructed from rate data between 348 and 393 K consistently yields a straight line. The apparent activation energy (which is a reflection of both mass-transfer and kinetic rates) calculated from the slope is between 28 and 31 kJ/mol.

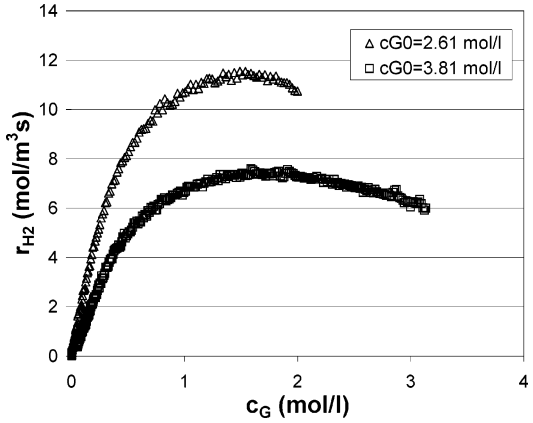

Figure 5. Comparison of rate profiles at different starting concentrations. Consecutive experiments using catalyst H at 393 K and 8.1 MPa. The shapes of the rate profiles, which exhibit a maximum rather than a plateau, were peculiar to catalyst H and were not observed with other catalysts.

Three experiments were conducted at 373, 383, and 393 K (and otherwise identical conditions). The apparent activation energy was evaluated from both the $r_{H_2,50\%}$ and k_1 measures of activity for each run, which yielded 38 and 43 kJ/mol, respectively. The trend that the apparent activation energy increases as the glucose concentration decreases may hold information on the reaction mechanism and/or its interaction with mass-transfer resistance.

In one experiment, the temperature was increased from 373 to 393 K to accelerate the reaction between 90% and 100% conversion. Using nonlinear regression, the entire rate profile for this experiment (between the time when the temperature reached 348 K in the initial heatup until the time of full conversion) was fit to eqs 1 and 2. The kinetic parameters k, K_G and n, and E_A were determined simultaneously. The resulting model fits the experimental data well. The value for the activation energy E_A was 33 kJ/mol. Extending the model to include the temperature dependence of K_G did not significantly improve the model fit.

Effect of the Glucose Concentration. The glucose concentration appears in rate expressions such as eq 1. According to most models found in the literature, the order of the reaction rate in glucose varies between 0 and 1. Indeed, individual batch rate profiles appear to confirm this dependence. An alternative way of exploring this is to vary the concentration of glucose in the aqueous solution charged to the reactor. With a positive order in glucose, the initial reaction rate at high-concentration runs should be high. In experiments conducted at 1.20, 2.60, and 3.82 mol/L glucose feeds, we found that, in fact, the reaction rate follows the opposite trend: the relative values of $r_{H_2,50\%}$ were 1.2, 1.0, and 0.7, respectively. Compared at points of equal glucose concentration, the relative rate differences are even more pronounced, as is evident from the relative values of k_1: 1.5, 1.0, and 0.6, respectively. These trends are illustrated in Figure 5, which compares rate profiles

Table 2. Comparison of Monolithic and Slurry Catalysts[a]

catalyst	supplier	P (MPa)	T (K)	c_{G0} (mol/L)	$r_{H_2,50\%}$ (mol/kg$_{Ru}$·s)	k_r (mol/MPa·kg$_{Ru}$·s)	E_A (kJ/mol)
			This Study				
monolithic HH	Johnson Matthey	8.1	393	2.61	0.75	0.13	34
Raney Ni	Grace 6800	5.6	413	2.61	0.07	n/d	n/d
5% Ru/C	Johnson Matthey	5.4	393	1.20	4.94	1.79	*b*
5% Ru/C	Johnson Matthey	5.6	393	2.61	7.43	1.37	*b*
5% Ru/C	Engelhard	5.8	393	2.61	4.03	0.99	*b*
			Comparative Data from Crezee et al.[6]				
5% Ru/C	Engelhard	4−7.5	393	0.56−1.39		1.30	73

[a] The monolithic data in the table is the best performance measured in our experiments. Rate measures for Raney nickel are relative to the nickel weight. Values for k_r derived by nonlinear regression at a constant value of $K_G = 1.8$ L/mol. [b] See text.

at 2.60 and 3.81 mol/L glucose. Several hypotheses may explain the decrease in the rate with concentration:

1. The higher viscosity of the high-concentration solution gives rise to a greater degree of mass-transfer resistance. This may be due to both the lower diffusivity of hydrogen in the viscous liquid (which would affect both external and internal mass transfer) and the lower rate of liquid circulation through the monolith (affecting only external mass transfer).

2. At some level of conversion, the sorbitol product inhibits the rate of reaction by competitive adsorption onto the catalyst active sites. Sorbitol does not appear in the kinetic expressions explored thus far: because most experiments were conducted at the same starting concentration, the sorbitol and glucose concentrations are not independent variables. Models such as eq 1 can easily be extended with a term in the denominator to account for this inhibition. However, this cannot explain the lower initial rates when sorbitol is not yet present.

3. Models where glucose has between 0 and 1 order reflect the assumption that hydrogen does not competitively adsorb on the catalyst surface. When $n > 1$ in eq 1, hydrogen competes for the same surface sites, and depending on parameter values, high glucose concentrations may inhibit the reaction. In fact, nonlinear regression of eq 1 to our results yields the best fit for $n > 1$, as is evident from Figure 2. Of course, this cannot explain why the rates at equal glucose concentration depend on the initial glucose concentration.

Most likely, the true reaction mechanism is quite a bit more complex than the simple models discussed so far, with glucose, hydrogen, and sorbitol all factoring into the kinetic rate expression, which is, in turn, modified by mass-transfer resistance. Note that our discussion here disregards the additional complexity due to glucose mutarotation equilibria, which may further complicate the analysis. While we have explored several extensions of the basic models expressed by eq 1, such as including terms for sorbitol or hydrogen adsorption, none was found to adequately describe our data. Without a more extensive set of experimental data in which the various factors are individually manipulated, we cannot further elucidate the mechanism.

The statistical results from nonlinear regression of eq 1 to our data show that k_r and K_G are strongly (negatively) correlated. Fixing the value of one to an average value and only determining the other does not significantly change the degree of fit. To facilitate comparison of experimental results, we chose to fix the value of K_G at 1.8 L/mol, the value reported by Crezee et al.[6]

Comparison to Slurry Benchmarks. Because process implementations of monolithic catalysts would differ substantially from current slurry practice (most notably in the number of batches completed using a single charge of catalyst), direct comparisons of the activity between slurry catalysts and monoliths do not have much economic relevance. However, the relative performance can elucidate more fundamental differences in kinetic and mass-transfer performance and also serve as a starting point for further optimization of monolithic catalysts.

We evaluated one Raney nickel catalyst (Grace 6800) but found that it had very little activity at 393 K. A more appropriate benchmark would have been Grace 3111, a molybdenum-doped Raney nickel that is commercially applied in sorbitol manufacture. Two 5% Ru/C slurry catalysts were used as benchmarks. One was obtained from Johnson Matthey and the other from Engelhard. Both were evaluated in a typical liter-scale laboratory hydrogenation reactor, at catalyst loadings from 2 to 5 g/L.

Comparative results are shown in Table 2, which includes data from a monolithic experiment and our slurry experiments, as well as parameters derived by Crezee et al.[6] from nine experiments conducted using 5% Ru/C at $T = 373-403$ K, $P = 4.0-7.5$ MPa, and $c_{G0} = 0.56-1.39$ mol/L. To compare activities of slurry and monolithic catalysts, both are normalized to their rate per kilogram of ruthenium metal measured at 393 K. To allow comparison with the results from Crezee et al., eq 1 with $n = 1$ and $K_G = 1.8$ L/mol was fit to experimental data. The activation energy for the monolith was discussed above. For the slurry catalysts, activation energies were derived from the initial ramp to 393 K. However, we found that the results differed depending on whether the catalyst used was fresh or reused; fresh catalyst yielded Arrhenius slopes corresponding to 30−35 kJ/mol, whereas two experiments using reused catalyst yielded 52 and 80 kJ/mol. We believe that this is indicative of a catalyst line-out phenomenon, which convolutes the temperature dependence. The higher values on reuse are in the same range as those reported by Crezee et al. All slurry experiments yield k_r values in the range 1.0−1.8 mol/MPa·kg·s, which we consider to be similar, given experimental error and an imperfect kinetic model. Significantly, the rate constant for Ru/C was higher at the glucose starting concentration of 1.2 L/mol than it was at 2.61 L/mol; this is consistent with the trend observed in monoliths.

Compared to all of the slurry results, the rate per amount of ruthenium was significantly slower for the monolithic catalysts: the ruthenium effectiveness of the monolith is about 10−15% that of the slurries. Several explanations may be offered for the lower ruthenium effectiveness of the monolith: lower ruthenium dispersion, lower turnover rate of ruthenium sites, or lower availability of reactants at the catalyst surface due to mass-transfer limitations. Metal dispersion for 5% Ru/C catalyst from Johnson Matthey was determined to be

45%. Dispersions of the calcined and noncalcined monoliths ranged from 11% to 41%, with little difference in the overall activity. Crezee et al.[6] report a 33% dispersion of the Ru/C catalyst they used. It appears, therefore, that Ru dispersion levels cannot explain the activity difference. Because precursors and metal deposition methods for carbon-based slurry catalysts are different from those for monolithic catalysts, it is certainly possible that the intrinsic activity of the ruthenium metal would be different as well. However, because the calcined and noncalcined monolithic catalysts, which should have rather differently structured ruthenium phases, exhibit similar activities, we consider it unlikely that this explains the large activity difference between the slurry and monolith. Most likely, mass-transfer limitation due to pore diffusion of hydrogen suppresses the monolithic activity. Certainly the fraction of the ruthenium that is contained in the thickened washcoat layer in the corners of monolithic channels is likely to contribute little to the overall effectiveness. Traditional effectiveness factor calculations require that the washcoat thickness and effective diffusivity are known. Calculations using rough estimates for these parameters at the standard conditions of our experiments yield effectiveness factors in the range of 0.2−0.5, which points to moderate mass-transfer limitation. Under conditions of internal mass-transfer control, the measured apparent activation energy is half of the true activation energy on the catalyst surface; this is close to the ratio between our measured activation energy and the value reported by Crezee et al., which is further evidence for internal mass-transfer limitation.

Conversion, Selectivity, and Byproducts

Glucose hydrogenation products were withdrawn from the reactor after cooldown. Almost invariably, they were colorless and odorless. Some colored products with a caramel aroma were produced in early experiments in which the reaction was taken to higher temperatures (140−160 °C). Reaction products remained clear even in extended storage, with no efforts to exclude air or light. This contrasts with typical commercial hydrogenation products, which emerge from the reactor slightly yellow. The final reactor product pH was usually between 3.7 and 5.

In intermediate samples, the measured concentration of glucose corresponded reasonably well to the concentration calculated from the hydrogen mass balance. However, the most important glucose measurement is that of residual glucose in the final product. The commercial specification for the final glucose concentration in the product is between 0.04 and 0.10 wt %, based on the tendency of residual glucose to form colored products in end-user applications of sorbitol. The HPLC method allowed glucose to be measured to levels well below these specification concentrations. However, in the analysis of product samples, the glucose measurement was overstated, possibly because of one or more small byproduct peaks that eluted at approximately the same time as glucose. We analyzed several samples for which the HPLC analysis reported approximately 0.2 wt % glucose using an enzymatic assay method. The glucose concentrations measured by this method were less than 0.05 wt %. Although we cannot report reliable final glucose concentrations, we conclude that the catalysts we studied are capable of reducing the glucose concentration to below the commercial specification level.

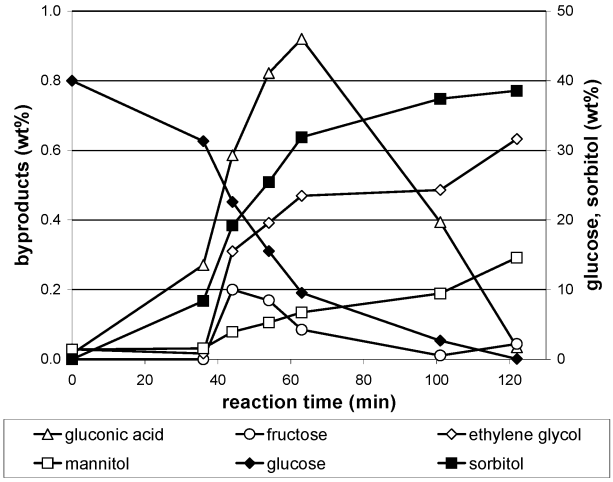

Figure 6. Concentrations of glucose, sorbitol, and byproducts as a function of experiment time (catalyst H, T = 393 K, P = 8.1 MPa, and c_{GO} = 2.61 mol/L).

A small amount of rinse water remained in the reactor between consecutive experiments. As a result, we cannot accurately calculate selectivity toward sorbitol from the sorbitol concentration measured in the product sample. Instead of selectivity, we will discuss the concentrations of byproducts measured by HPLC.

The byproducts most likely to affect the overall selectivity are gluconic acid, fructose, mannitol, ethylene glycol, and glycerol. Other possible byproducts include isomers of sorbitol such as galactitol and iditol and other sugar alcohols such as arabitol and ribitol. Using prepared standards, we were able to identify gluconic acid, mannitol, fructose, and ethylene glycol.

Gluconic Acid. In slurry catalyst experiments using Raney nickel, the concentration of gluconic acid increased and then stabilized to a constant level. For ruthenium slurry and monolithic catalysts, in contrast, the gluconic acid concentration was found to go through a maximum: it is created during the initial stages of the batch and starts disappearing during the later stages. Concentrations of gluconic acid in solutions prepared using the Aldrich glucose feedstock never exceeded 0.02%. In intermediate samples from monolithic catalyst experiments, concentrations of gluconic acid ranged from 0.06 to 0.95%. Figure 6 plots the concentrations of glucose, sorbitol, and various byproducts in intermediate samples collected during one experiment. Gluconic acid is clearly formed during the time in which the bulk glucose is being converted. At some point, its rate of disappearance (by irreversible adsorption or chemical reaction) starts exceeding its rate of formation; by the time the glucose is fully converted, gluconic acid has also returned to a very low concentration.

Gluconic acid can be formed by dehydrogenation or oxidation of glucose. The dehydrogenation reaction is base-catalyzed.[5] During all reaction batches, the pH decreased from its initial value of around 6 to final values of around 4. The decrease is most likely due to the formation of gluconic acid and would serve to suppress base-catalyzed reactions. Glucose oxidation (possibly catalyzed by ruthenium) can occur if the feed solution contains dissolved oxygen. Arena[8] identified this as a source for ruthenium catalyst deactivation in fixed-bed hydrogenation of glucose. In most cases, the deionized water used to prepare glucose solutions was

deoxygenated by sparging with nitrogen, but no effect of this treatment was noted in the catalyst activity or selectivity. Hence, the mechanism by which gluconic acid forms is not clear. Perhaps the catalyst washcoats maintain some level of surface alkalinity that serves to catalyze glucose dehydrogenation to a small extent.

Fructose and Mannitol. Fructose can be formed by isomerization of glucose. This reaction is also base-catalyzed and would not occur to any significant extent at the pH levels described above. Indeed, fructose is not seen in high concentrations in samples from the laboratory experiments. Fructose is itself hydrogenated, yielding sorbitol and mannitol, by catalysts active toward glucose hydrogenation, albeit at a lower rate. Heinen et al.[11] demonstrated in fructose hydrogenation experiments at 72 °C that at those conditions glucose adsorbs much more strongly to Ru catalysts than fructose, leading to an inhibition of the hydrogenation of fructose. Figure 6 shows that both gluconic acid and fructose are produced during the experiment and reach a maximum concentration before they start to decline. Fructose reaches its maximum well before gluconic acid does, most likely because its hydrogenation proceeds more rapidly.

In experiments where the glucose was sufficiently converted, fructose concentrations did not exceed 0.01% in the final product. Therefore, the ultimate byproduct resulting from fructose formation is mannitol. We would expect mannitol to be formed at concentrations of the same order of magnitude as the maximum fructose concentration observed in intermediate samples. Indeed, Figure 6 shows that about 0.3% mannitol was formed. This is typical of final samples for all experiments, which contained 0.1−0.3 wt % mannitol. The limited data available from experiments where the temperature exceeded 393 K suggest that the mannitol peak area increases with temperature. Because mannitol and glycerol coelute, the source of this increase may, in fact, be glycerol produced by high-temperature cracking.

Ethylene Glycol. Because of its toxicity, ethylene glycol is a more troubling byproduct than most. In most experiments, it accumulated to a concentration of 0.2−0.4 wt % in the final product. From series of intermediate samples, it appears to be formed throughout the batch hydrogenation, not just when glucose is mostly converted. As with mannitol/glycerol, there is a slight positive correlation between the reaction temperature and glycol formation.

Unidentified Byproducts. Several additional compounds appear in the chromatograms. Most prominently, in experiments conducted at higher temperatures or extended reaction times, an additional unidentified byproduct was observed as a shoulder on the tail of the sorbitol peak. Attempts to identify the compound giving rise to the "over-temperature" peak by liquid chromatography−mass spectrometry and gas chromatography−mass spectrometry were not successful, so it is identified here as the "over-temperature byproduct".

Effect of Extended Batch Time. Most byproducts are formed in the low concentration ranges mentioned above (several tenths of a percent) by the time the glucose is converted to the specification level. However, when the batch time is extended beyond that point, byproduct formation accelerates, as illustrated in Figure 7. Mannitol/glycerol and the over-temperature byproduct are formed especially rapidly, while glycol and "other" byproducts continue to form at a more moderate rate. At the same time, the sorbitol concentration decreases. Clearly, holding sorbitol solutions at the process temperature and pressure in the presence of the monolithic catalysts results in degradation of the sorbitol.

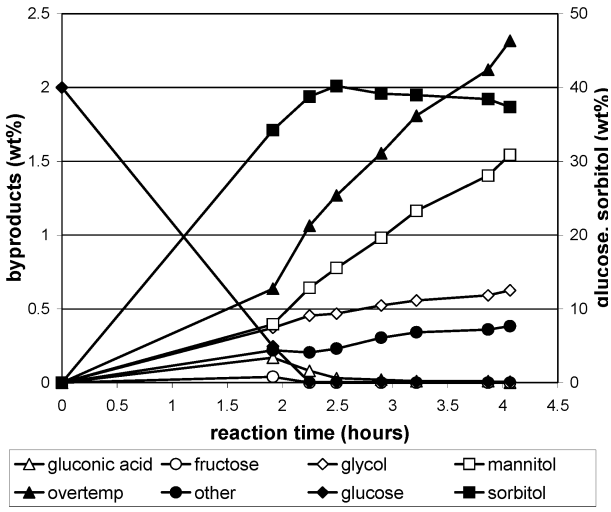

Figure 7. Concentrations of glucose, sorbitol, and byproducts during an experiment using catalyst H at $P = 6.2$ MPa, $T = 393$ K, and $c_{G0} = 2.61$ mol/L. The accumulation rate for most byproducts accelerates when most of the glucose has been converted, while the sorbitol concentration decreases.

Comparison to Slurry Results. Reaction products from experiments using 5% Ru/C were also analyzed by HPLC. The total byproduct make for the slurry experiments was generally lower than that for the monolithic experiments, mostly because of much lower mannitol concentrations (<0.1 wt %). Gluconic acid and glycol concentrations were also somewhat lower. The higher byproduct make for monolithic catalysts may be caused by support effects or by the lower hydrogen availability at the catalyst surface due to mass-transfer limitations.

Catalyst Stability

Life Testing. Several catalyst formulations were subjected to multiple repeated runs at varying process conditions, periodically returning to the standard conditions. In these series of experiments, the catalyst activity declined slowly but steadily. In one series, catalyst A lost about 25% of its initial activity over the course of 14 runs. The partly deactivated catalyst was analyzed and compared to a sample of the fresh catalyst. Microscopy (optical and scanning electron) did not uncover any changes in catalyst morphology. The crystallite size measured by X-ray diffraction was 35% larger in the used sample than in the fresh sample; this difference may be within experimental error. However, if the difference indicates a real crystallite growth, then the corresponding reduction in the surface area would be 45%, enough to explain the activity loss. Other measures, such as the BET surface area and average pore diameter, did not change significantly.

Catalyst H was subjected to 43 consecutive batch runs. Almost all runs were conducted at the standard conditions (80 barg, 120 °C); for a few runs toward the end of the series, the temperature was ramped up to 130 or 140 °C toward the end of the run or was maintained at the higher temperature for the entire duration. Figure 8 shows the progression of both measures of catalyst activity as a function of the run

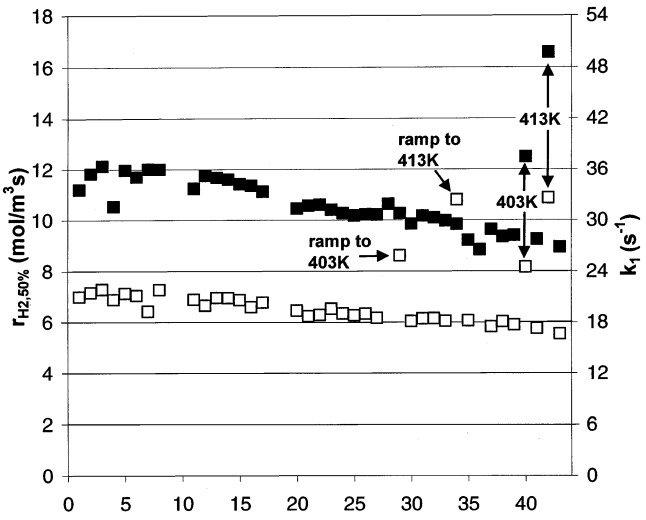

Figure 8. Activity of catalyst H through a 43-experiment life study. Except where noted, conditions were $T = 393$ K, $P = 8.1$ MPa, and $c_{G0} = 2.61$ mol/L. Solid squares represent $r_{H_2,50\%}$, and open squares, k_1.

number. The measures correlate well with each other, except where the temperature was ramped toward the end, in which case k_1 is disproportionately higher, as expected. Both measures show a slow but steady decline, each losing about 20% of its initial value by the 43rd batch. The series was not run out long enough to discern whether the rate would stabilize or proceed at a lower rate of decline at large numbers of reuses.

Several causes for the deactivation may be at play. Because gluconic acid is present in intermediate reaction samples, it may act as a catalyst poison.[8] Heavy metals such as iron have also been implicated; iron contamination in the cordierite substructure complicates measurement of iron accumulation on the catalyst, so this has not been evaluated. Other possibilities are hydrothermal rearrangement of the ruthenium and/or the ceramic washcoat and deposition of heavy organics on the catalyst surface.

Effect of the Temperature. Although it is not evident from Figure 8, evidence from shorter series of experiments conducted with other catalysts suggests that catalyst deactivation is accelerated by operation at temperatures above 120 °C. Because high temperature facilitates most of the possible causes for deactivation mentioned above (e.g., formation of gluconic acid or caramelization byproducts, dissolution of iron, or hydrothermal processes), this does not elucidate the mechanism for deactivation. However, it suggests that an optimized process must carefully control and manipulate the temperature to maximize the rate of reaction while avoiding excessive catalyst deactivation.

Metal Leaching. The products from benchmarking experiments using Raney nickel contained nickel, iron, and aluminum at concentrations of about 30 ppm. This is consistent with industrial practice, where nickel leaching poses a significant issue. Products from experiments using ruthenium catalysts (both slurry and monolith) contained much lower metal levels, with both iron and ruthenium at <30 ppb. Aluminum is still present at ppm levels, presumably because of leaching from the cordierite monolithic structure.

Final Discussion and Conclusions

In extensive laboratory testing of various monolithic catalyst formulations, we have demonstrated that ruthenium monolithic catalysts can satisfactorily convert glucose to sorbitol at conditions similar to those currently used in commercial production processes. The reaction rates demonstrated are 5−10 times lower than the rates obtained with slurry ruthenium catalysts (on a ruthenium mass basis) but are sufficiently high to render a monolith-based process economically attractive (economic considerations are discussed in more detail by Machado et al.[9]). Several formulations were subjected to life testing (tens of consecutive runs), during which a slow but significant rate of activity loss was noted. The cause for the decreasing activity has not yet been established; possible causes include poisoning by gluconic acid, iron, or high-molecular-weight byproducts or rearrangement of ruthenium or washcoat materials under the influence of temperature and/or acidic conditions. Our results suggest that catalyst optimization is likely to yield further improvements in the areas of catalyst activity and stability.

The monolithic catalysts exhibited conversion and selectivity levels that meet commercial specifications. Primary byproducts were gluconic acid, mannitol, and ethylene glycol, at concentrations of 0.1−0.4 wt %. Fructose and several unidentified byproducts were found at lower concentrations. Byproduct formation was accelerated after the glucose was substantially converted. Unlike in stirred-tank slurry reactors, in a monolith loop reactor contact between the reaction product and catalyst could be easily ceased after this point is reached. Residual glucose could be readily reduced to below the commercial target of 0.04 wt %. The concentration of ruthenium in the reaction product due to catalyst leaching was about 30 ppb, a 1000-fold decrease from the nickel levels seen with a Raney nickel catalyst. Since the completion of this laboratory study, we have completed a pilot study using several of the catalysts discussed here; the specific rates obtained in the laboratory were reproduced at the pilot scale. More details will be presented elsewhere.

In summary, processes centered on monolithic catalysts appear to be attractive in the area of sugar alcohol hydrogenation. These catalysts can likely be optimized beyond the first generation described here to further improve the rate and stability performance and thereby render commercial implementation even more attractive.

Acknowledgment

We gratefully acknowledge the support from Johnson Matthey Catalysts, who prepared the monolithic catalysts and conducted pre- and postreaction catalyst characterization.

Nomenclature

c_G = glucose concentration (c_{G0} is the initial concentration), mol/L
E_A = apparent activation energy (temperature dependence of k_r), kJ/mol
k_1 = slope of rate vs glucose concentration curve, between 90% and 100% conversion, s^{-1}
K_G = glucose adsorption coefficient, L/mol
k_r = lumped kinetic parameter in the LHHW-type rate model, normalized either by the volume of the monolithic catalyst or by the mass of the catalytically active metal [mol/MPa·m^3·s or mol/MPa·kg·s]
n = exponent in the LHHW-type rate model
P = total pressure (absolute), MPa

p_{H_2} = hydrogen partial pressure, MPa
R = gas constant, J/mol·K
r_{H_2} = reaction rate normalized per volume of monolithic catalyst or mass of catalytically active metal [mol/m^3·s or mol/kg·s]
$r_{H_2,50\%}$ = r_{H_2} averaged between 40% and 60% glucose conversion, normalized to 8 MPa·g pressure [mol/m^3·s or mol/kg·s]
T = reaction temperature, K

Greek Letters

ξ = conversion

Literature Cited

(1) Cybulski, A.; Stankiewicz, A.; Edvinsson Albers, R. K.; Moulijn, J. A. Monolithic reactors for fine chemicals industries: a comparitive analysis of a monolithic reactor and a mechanically agitated slurry reactor. *Chem. Eng. Sci.* **1999**, *54*, 2351−2358.

(2) Heiszwolf, J. J.; Engelvaart, L. B.; van den Eijnden, M. G.; Kreutzer, M. T.; Kapteijn, F.; Moulijn, J. A. Hydrodynamic aspects of the monolith loop reactor. *Chem. Eng. Sci.* **2001**, *56*, 805−812.

(3) Machado, R. M.; Broekhuis, R. R. Gas−liquid reaction process including ejector and monolith catalyst. U.S. Patent 6,506,361, Jan 14, 2003.

(4) Broekhuis, R. R.; Machado, R. M.; Nordquist, A. F. The ejector-driven monolith loop reactor−experiments and modeling. *Catal. Today* **2001**, *69*, 87−93.

(5) De Wit, G.; de Vlieger, J. J.; Kock-van Dalen, A. C.; Heus, R.; Laroy, R.; van Hengstum, A. J.; Kieboom, A. P. G.; van Bekkum, H. Catalytic dehydrogenation of reducing sugars in alkaline solution. *Carbohydr. Res.* **1981**, *91*, 125−138.

(6) Crezee, E.; Hoffer, B. W.; Berger, R. J.; Makkee, M.; Kapteijn, F.; Moulijn, J. A. Three-phase hydrogenation of D-glucose over a carbon supported ruthenium catalyst−mass transfer and kinetics. *Appl. Catal. A* **2003**, *251*, 1−17.

(7) Nijhuis, T. A.; Beers, A. E. W.; Vergunst, T.; Hoek, I.; Kapteijn, F.; Moulijn, J. A. Preparation of monolithic catalysts. *Catal. Rev.* **2001**, *43*, 345−380.

(8) Arena, B. J. Deactivation of ruthenium catalysts in continuous glucose hydrogenation. *Appl. Catal. A* **1992**, *87*, 219−229.

(9) Machado, R. M.; Broekhuis, R. R.; Heiszwolf, J. J.; Carney, S. R. Practical considerations in using monolith catalysts in gas−liquid reaction processes. In preparation, expected publication date 2004.

(10) Vanoppen, D.; Maas-Brunner, M.; Kammel, U.; Arndt, J.-D. Process for making sorbitol. World Patent Application 02/100539A2, Dec 12, 2002.

(11) Heinen, A. W.; Peters, J. A.; van Bekkum, H. Hydrogenation of fructose on Ru/C catalysts. *Carbohydr. Res.* **2000**, *328*, 449−457.

Received for review January 29, 2004
Revised manuscript received May 12, 2004
Accepted May 12, 2004

IE0400393